

MONITORING LANDSLIDE DISPLACEMENTS DURING A CONTROLLED RAIN EXPERIMENT USING A LONG-RANGE TERRESTRIAL LASER SCANNING (TLS)

J. Travelletti^{a*}, T. Oppikofer^b, C. Delacourt^c, J.-P. Malet^a, M. Jaboyedoff^b

^a School and Observatory of Earth Sciences, EOST, UMR 7516 CNRS, University Louis Pasteur, France - (julien.travelletti, jeanphilippe.malet)^a@eost.u-strasbg.fr

^b Institute of Geomatics and Risk Analysis (IGAR), University of Lausanne, Switzerland - (thierry.oppikofer, michel.jaboyedoff)^b@unil.ch

^c European Institute of Marine Studies, University of Western Britain, Brest, France - christophe.delacourt^c@univ-brest.fr

Commission V, Working Group V/3

KEY WORDS: Remote sensing, landslide, Laser scanning, Monitoring, Image correlation

ABSTRACT:

A controlled rain experiment has been performed on the Super-Sauze mudslide (South French Alps) in order to better understand the hydrology and mechanics of such type of landslides. The rainfall experiment was conducted during several consecutive days on a plot of about 120 m². The landslide displacements were monitored by Terrestrial Laser Scanning (TLS) during 5 days from July 10-14, 2007 with one scan acquisition per day. The scans were fitted on a stable slope outside the rain area. Three techniques were used to characterize the displacements: the benchmark method, the cloud to cloud comparison method and the shaded relief image correlation method. All techniques indicate an average displacement rate of 3.2 cm.day⁻¹ with a slight acceleration on day 3. The benchmark method allowed to identify the direction of sliding and thus to estimate the dip of the slip surface. Information on the velocity vertical profile can also be derived from the benchmark method.

1. INTRODUCTION

In the South French Alps, the Callovo-Oxfordian clay-shales (e.g. black marls) of the Ubaye Valley present a high susceptibility to weathering and erosion. The landscape is severely affected by many shallow and deep-seated landslides. Among them, the Super-Sauze mudslide is being studied since 10 years to gain more understanding on the factors and mechanisms controlling the behaviour of landslides developed in clay shales.

The Super-Sauze mudslide (Figure 1) is a flow-like landslide characterized by a complex vertical structure associating a slip surface and a viscoplastic plug. Multidisciplinary observations (geology, geomorphology, geotechnics, hydrology; Flageollet *et al.*, 1999) provide substantial information about its geology and geometry. The mudslide material consists of a silty-sand matrix mixed with moraine debris. It extends over an horizontal distance of 850 m and occurs between an elevation of 2105 m at the crown and 1740 m at the toe with an average 25° slope. Its total volume is estimated at 750,000 m³ and creeping velocities range from 0.01 to 0.04 m.day⁻¹ (Malet *et al.*, 2002). These displacements are spatially very variable over all the mudslide, and directly correlatd with the geometry of the covered paleotopography and the presence of water. The paleotopography plays an essential role in the behaviour of the mudslide by delimiting preferential water and material pathways and compartments with different kinematic, mechanical and hydrodynamical characteristics (Malet and Maquaire, 2003). The rate of displacement is directly controlled by the hydrological regime and period of high water levels.

Within most of the year, the mudslide is characterized by nearly saturated conditions.

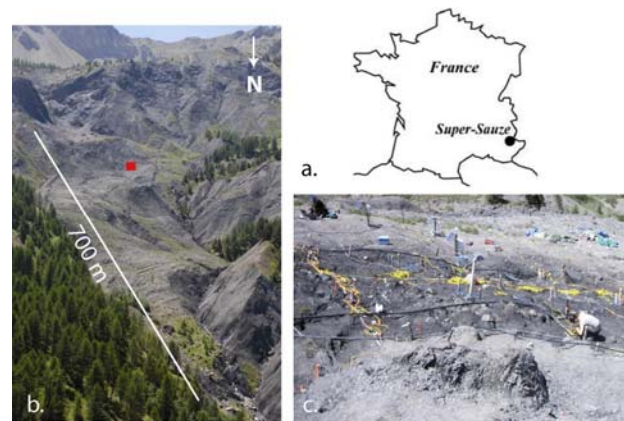


Figure 1. (a) Location of the Super-Sauze mudslide. Aerial view of the mudslide in 2007 and location of the rain experiment (square). (c) Setup of the rain experiment area

In order to better understand the factors controlling the hydrology and the mechanics of the mudslide, a rain infiltration experiment has been conducted in July 2007 (Figure 2). This experiment consisted in applying rain on a representative plot of about 120 m² (7 x 14 m) during 4 consecutive days. The rain consisted in water enriched in chloride and bromide and a rain intensity of 15 mm.h⁻¹ was applied. Geophysical (electrical

* Corresponding author.

resistivity, P-wave velocity), hydrological (soil water content, soil suction, groundwater level, water discharge, soil temperature) and hydrochemical parameters (water quality, water conductivity) were observed before, during, and after the rain experiment at several locations within the experiment plot (Figure 2). The focus of this paper is on the characterization of the landslide kinematics by using a Terrestrial Laser Scanning technology.

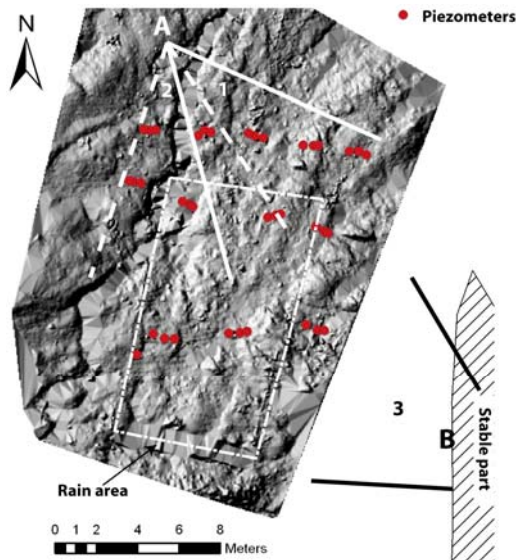


Figure 2. Map of the rain experiment plot and location of the 31 piezometers installed at different depths. Three laser scans were acquired from two viewpoints (A and B) to cover the entire rain plot.

2. METHODOLOGY OF DISPLACEMENT MONITORING

2.1 Terrestrial Laser Scanning technology

The displacement monitoring equipment used in this study is a long-range terrestrial laser scan (TLS) which principle is based on the time-of-flight distance measurements using an infrared laser (Slob and Hack, 2004). This technology is very interesting for monitoring slope displacements because it provides a rapid collection of field topographical data with a high density of points (Rosser et al., 2007; Conforti et al, 2005; Abellan et al, 2006; Monserrat and Crosetto, 2008; Oppikofer et al, 2008).

For the present study, the displacements were monitored by a Optech ILRIS-3D TLS system with a wavelength of 1500 nm. The monochromatic and nearly parallel laser beam is sent out in a precisely known direction. The pulse is back-scattered by the terrain and by several man-made objects such as the piezometer tubes installed on the site, and then recorded by the acquisition system. Knowing the speed of light, the travel time of the signal is then converted into the distance between the scanner and the object. Finally the Cartesian coordinates as well as the intensity of the beam (which is dependant of the object reflectivity) are registered. Mirrors inside the scanner allow the acquisition of a 40° wide and 40° high field of view in a single acquisition with about 2500 pts.s^{-1} . The 3D coordinates of each point are defined by its distance and direction from the scanner. The range of the used TLS is usually up to 800 m. On the field, the scanning

range is difficult to evaluate because the effect of the atmosphere and soil moisture can significantly decrease the reflectivity of the target (Rosser et al., 2007). The resolution depends on the distance to the objects and on the chosen angular spacing between two spots.

1.1 Data acquisition

Displacements during the rain experiment were monitored by time series of TLS point clouds, with an acquisition per day. In order to obtain a complete topographical model of the terrain and of the objects (piezometers, benchmarks) minimizing the shadow zones, three consecutive scans from different viewpoints were carried out (Figure 2). TLS point clouds were acquired from almost the same position and orientation over 4 days from July 10-14, 2007 at noon. The rain experiment was interrupted during the scanning. Ground control points were positioned in the mudslide but outside the rain experiment plot. This ground control points consisted in white CD (diameter of 12 cm) fixed on black and white sticks. Their positions were measured with a DGPS in order to georeference the 3D images.

For the multi-temporal analysis, it was essential to include stable areas into the scanned area (Monserrat and Crosetto, 2008). The three individual scans were then combined using first a manual alignment procedure, and second an automated iterative procedure in order to minimize the alignment error. However, each acquisition has its own reference system. Therefore, they were matched over the stable areas and compared with the reference (first acquisition). All the processing was performed with the Polyworks software (<http://www.innovmetric.com>).

2.2 Displacement characterization and quantification

The displacements were characterized by comparing the acquisition of the first day (reference) with the point clouds of the following days. Three methods were used to quantify the displacement from the original point clouds.

a) The benchmark method (M1): the movement of several objects (e.g. blocks of marls, piezometers, etc) allowed to precisely compute the direction of displacements because the scans from different viewpoints provide a complete 3D description of the objects. For instance, each piezometer can be modeled by fitting a cylinder on the point cloud (Figure 3). The boundaries of the cylinders were determined for 31 piezometers for each scan acquisition. The vectors between the cylinder boundaries of two consecutive dates provide the direction and the amplitude of the displacement. The rebuilding of the piezometer geometry was considered accurate if the diameter of the fitted cylinder is equal to $5 \pm 1 \text{ cm}$. For the area outside the rain experiment plot, a TIN (Triangulated Irregular Network) model was realized on 9 representative blocks. This technique allows to take into account the translational and rotational displacements of all the data points (Monserrat and Crosetto, 2008; Oppikofer et al, 2008).

A 4×4 matrix expresses then the affine transformation of the object geometry at different dates: 9 terms for the rotation, 3 terms for the translation (Stephens, 2000).

b) Cloud to cloud comparison method (M2a-b) : the function "shortest distance" (M2a) available in *Polyworks* consists in computing for each point of a point cloud the distance to its nearest neighbor in the reference point cloud. This method is

particularly useful when the direction of movement is unknown, but has the disadvantages of producing non reliable results because of the rough comparisons between two point clouds. Therefore, the amplitudes of displacement have been computed along the displacement vectors (M2b) determined from the 31 piezometers.

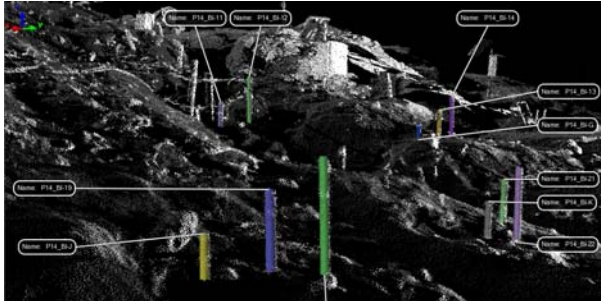


Figure 3. Cylinder fitting on the piezometer point clouds

c) Correlation of shaded relief images (M3): the 2D displacement field of the terrain can be derived by correlating two optical images obtained at different time. This methodology has been applied on aerial and satellite images to measure the displacements generated by earthquakes (van Puymbroeck et al., 2000), landslides (Delacourt et al., 2004) and glacier flow (Kääb, 2002). The image correlation technique is based on the automatic identification of same textures within an image. On stable areas, visible ground features should be superimposed on two successive images. On areas characterized by movements, the visible and recognizable features are shifted by the displacements. In order to quantify the ground displacements, a correlation window is defined on the reference (often the oldest) image. The corresponding window is searched on the second image by maximizing a correlation function (Vadon and Massonnet, 2000, Baratoux et al., 2001). The starting point of the search is the expected position of the window as if no displacement occurred between two acquisitions. The measured shift is directly related to the ground displacement times the pixel size. The process is repeated for each pixel of the reference image. The result is composed of 3 arrays of the same size as the correlated images. The first array contains the shift in lines for each pixel, the second array contains the shift in columns, and the third array indicates the quality of the correlation. The variation of the soil surface state is a factor that deeply influences the quality of the correlation.

The method was applied on shaded relief image of DEMs computed by a linear triangulation of the TLS point clouds assuming a lambertian behaviour of the topography with a cell size of 5 cm. The sun elevation and azimuth parameters are chosen in order to maximize the contrast of the shaded image.

2.3 Characterization of the errors

a) Influence of soil moisture. In order to determine if the soil moisture of the topsoil has a significant influence on the TLS measurements accuracy, some tests were performed. A small plot of marls (~1 m²) was progressively wetted while several scans were acquired at a distance of 30 m. Then, the parts of each scan remaining dry were aligned on the reference with an fitting error < 1 cm). After determination of the difference between the data points (~ 3000 pts) of the scans, the mean values (0.3 cm) and the standard deviation (0.2 cm) between the

two scans are minimal. Consequently, the soil moisture has a minor impact on the accuracy of the measurements.

b) Influence of scan assembling. For the benchmark method, the alignment error of the three scans of day+1,+2 and +3 compared to the reference scan is of 1.1 cm ($\sigma < 1.0$ cm). for the cloud to cloud method, the comparison between the point clouds is based on the discrepancy of the alignment of the point clouds on the stable areas of the scans, and the mean error is 0.8 cm ($\sigma = 0.6$ cm).

c) Accuracy of the shaded relief image correlation. The theoretical accuracy of the method is better than 1/1'000 of pixel (i.e. 0.05 mm for a pixel size of 5 cm, Baratoux et al, 2001). However, the real accuracy depends (i) on the accuracy of the DEM geometry, (ii) on the point cloud density and repeatability and (iii) on the presence of shadows. The accuracy of the DEM geometry is related to the error in the repositioning of the scan points for each acquisition. As the TLS acquisition is not realized at the nadir, some shadows will mask part of the correlated area. The accuracy, estimated by averaging the displacement values in the stable area, is respectively of 2.3 cm ($\sigma = 1.8$ cm), 2.5 cm ($\sigma = 1.1$ cm) and 3.0 cm ($\sigma = 1.4$ cm) for respectively the 11 July, 13 July and 14 July 2007 acquisitions.

3. ANALYSIS OF THE MOVEMENT PATTERN

3.1 Movement pattern of the benchmarks

The sliding direction is identified towards 027°/30° ($\sigma = 6.0^\circ$) (Figure 4). The comparison with the reference scan indicates a displacement pattern larger than the accuracy of the method (Table 1). A slight acceleration is noticed for the last days with a mean daily velocity of 2.7 cm.day⁻¹ between the 11 and 13 July and 3.9 cm.day⁻¹ between the 13 and 14 July.

The displacements computed with the block analysis outside the rain experiment plot indicate that the amplitudes of the displacement are similar to those inside the rain experiment plot.

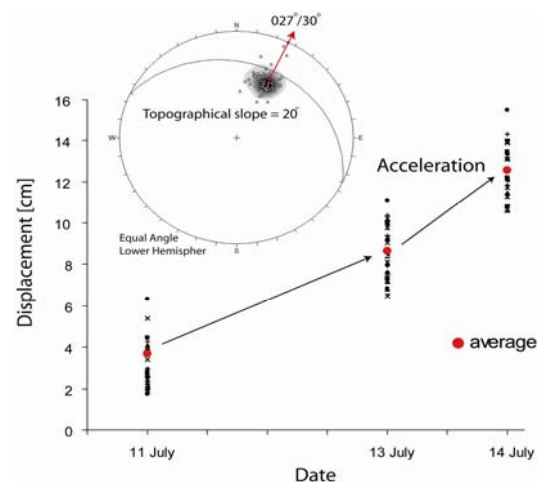


Figure 4. Amplitude and direction (lower hemisphere density stereonet representation) of displacement of 31 piezometers inside the rain experiment plot.

3.2 Movement pattern identified with the cloud to cloud method

A marked relief is needed to reliably detect displacements: terrain perpendicular to the main displacement vectors displays the highest contrast of displacement; inversely, no realistic displacements can be determined for terrain parallel to the main displacement vectors.

The “shortest distance function” indicates displacements affecting both the mudslide and the infiltration plot (Figure 5). However, the computed amplitudes of displacement are less than the displacements computed with the benchmark method (Table 1).

By taking into account the direction of displacement ($027^{\circ}/30^{\circ}$), the displacement field can be computed directly along the

vector. These displacements are larger than the one calculated with the shortest distance function (Table 1).

3.3 Relief image correlation method

The shaded relief image correlation method indicates also an increase of the horizontal displacement with time. The limit of the active area is clearly visible on the maps (Figure 6). Along the profile P1 crossing a stable area and the mudslide, average displacements of the mudslide context respectively 3 cm ($\sigma = 2$ cm), 6 cm ($\sigma = 2$ cm) and 11 cm ($\sigma = 2$ cm) are computed for respectively the 11, 13 and 14 July. The displacements of the piezometers inside the rain experiment plot showed an important spatial variability which is likely due to the method uncertainty (Table 1 and Figure 7).

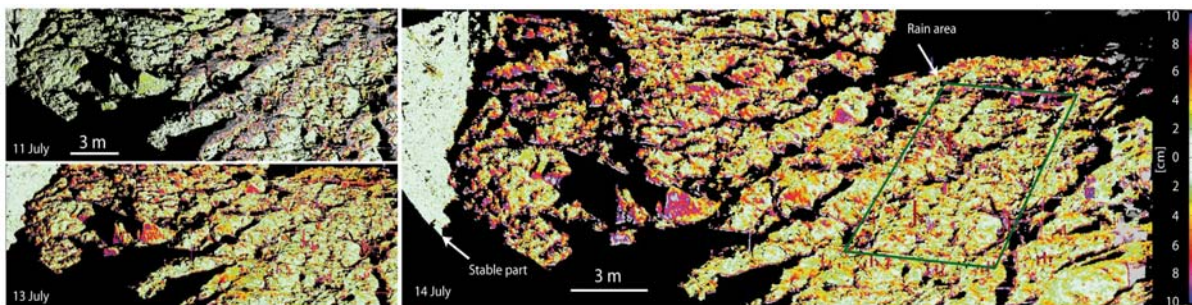


Figure 5. Displacements maps for the 11 July, 13 July and 14 July calculated with the “shortest distance” function.

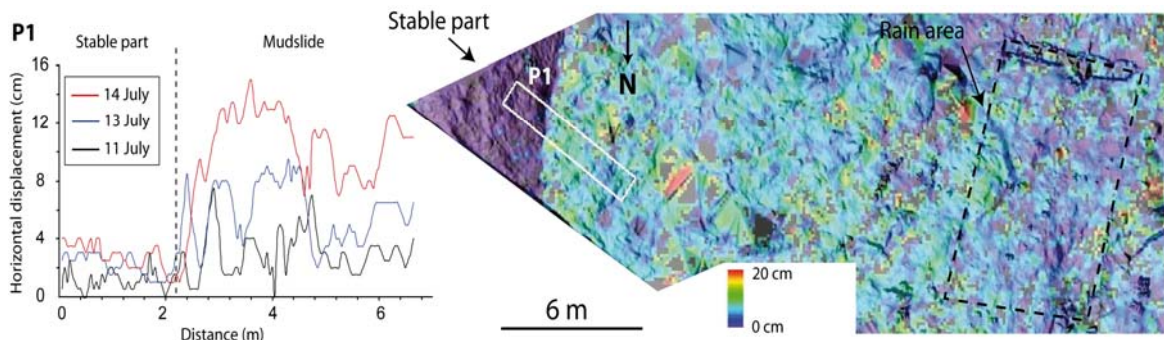


Figure 6. Displacement calculated from 10 to 14 July with the shaded relief image correlation technique. Profile P1 indicates the increasing displacements with time of the mudslide (on the East) in comparison to the stable part (on the West)

	11 July	13 July	14 July
M1	$\mu = 3.2$ cm $\sigma = 0.8$ cm	$\mu = 8.7$ cm $\sigma = 1.2$ cm	$\mu = 12.6$ cm $\sigma = 1.3$ cm
M2a	$\mu = 1.9$ cm $\sigma = 1.1$ cm	$\mu = 5.0$ cm $\sigma = 2.0$ cm	$\mu = 7.2$ cm $\sigma = 2.7$ cm
M2b	$\mu = 2.2$ cm $\sigma = 0.8$ cm	$\mu = 6.9$ cm $\sigma = 2.5$ cm	$\mu = 9.9$ cm $\sigma = 3.1$ cm
M3	$\mu = 3.2$ cm $\sigma = 2.0$ cm	$\mu = 7.1$ cm $\sigma = 2.1$ cm	$\mu = 9.5$ cm $\sigma = 2.2$ cm

Table 1. Average (μ) and standard deviation (σ) of the piezometer displacements calculated with the benchmark technique (M1) the point cloud “shortest distance” (M2a) and “along a vector” (M2b) function and the shaded relief image correlation method (M3)

4. DISCUSSION

4.1 Comparison of techniques

There is no correlation among the displacements calculated with the benchmark method and with the shaded relief image correlation method; this is probably linked to the uncertainty of the correlation due to the presence of shadow zones in the (Figure 7). However, the correlation of the daily average displacements is better and both methods indicate an increase in the displacement rate with time. Globally, the average displacements processed with the correlation method are systematically lower than those processed with the benchmark technique, probably because the displacements calculated with the shaded relief image correlation methods are in 2D.

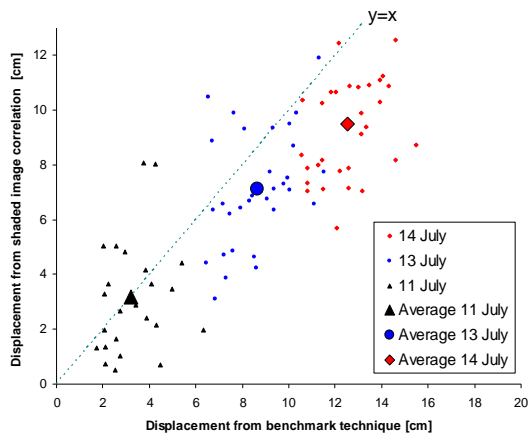


Figure 7. Comparison of the displacements of the 31 piezometers processed with the benchmark method and with the shaded relief image correlation method.

The point cloud method using the “vector” function (M2b) provides the displacements that are the closest to the benchmark method (Figure 8). Indeed, the “shortest distance” (M2a) function underestimates the displacements.

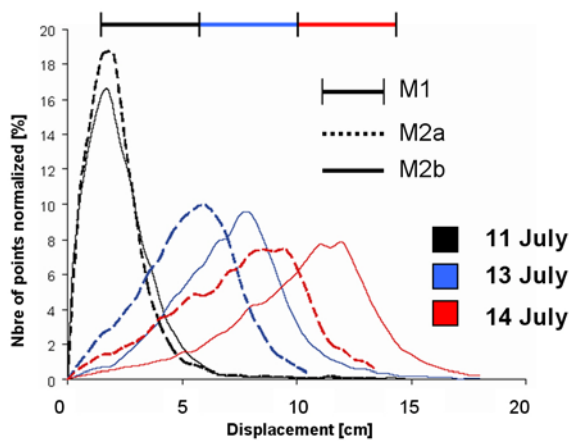


Figure 8. Histogram of displacements for the 31 piezometers with the techniques M1 and M2a-b

4.2 Analysis of the mudslide kinematics

By comparing the displacement computed by TLS with the displacement data monitored by an extensometer (Malet et al., 2002) located close to the infiltration area, the displacement amplitude can be validated (Figure 9). The extensometer indicates an acceleration of the mudslide in July 2007 and the TLS monitoring was performed at the beginning of this acceleration period. From the extensometer data, it cannot be concluded whether the increase in displacement rate is related to additional water inputs to the infiltration area or to a general acceleration of the entire mudslide body.

The dip of the slip surface may explain also why such high displacements affect the infiltration plot. The inclination of the displacement vector is steeper than the inclination of the topographical surface (Figure 4). From the monitoring of the inclination of the piezometers, it can be concluded that the vertical velocity profile is constant over the first 3 m (Figure

10), which is in agreement with the observed inclinometer data (Malet and Maquaire, 2003).

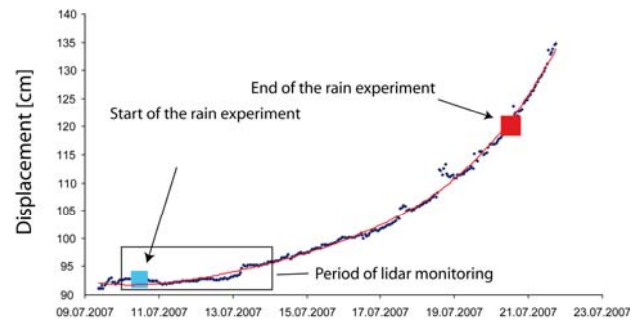


Figure 9. Displacement rate monitored by an extensometer located close to the infiltration plot.

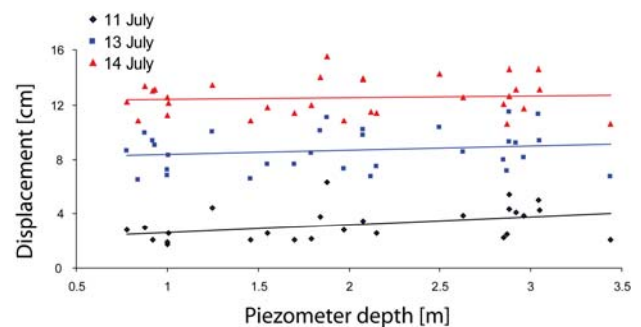


Figure 10. Relation between piezometer depths and their displacement through time.

5. CONCLUSION

TLS monitoring is a powerful technology to detect slope movements over a whole landslide area, but some careful precautions have to be taken into account while acquiring the data in the field. This study demonstrates especially the absolute need to calibrate the scans on stable areas to maximize the accuracy.

From a technical viewpoint, cloud to cloud comparisons give a good approximation of the displacement amplitudes provided that the terrain is the most perpendicular as possible to the sliding direction. Shaded relief image correlation is an interesting alternative if the TLS scans are systematically done at the same spot with a good resolution to discriminate topographical objects. However, the benchmark technique on rebuilt objects is the most reliable method to identify both the direction and amplitude of displacements.

From a thematic viewpoint, TLS monitoring allow to measure average displacement of 3.2 cm.day^{-1} in the direction $027^\circ/30^\circ$, and to estimate the dip of the slip surface ($\sim 30^\circ$). The dip of the slip surface explains partially the large displacement rates of this part of the mudslide.

ACKNOWLEDGEMENTS

This work was supported by the European Commission under the Marie Curie Contract 'Mountain Risks: from prediction to management and governance' (MCRTN-035798) and by ANR (France) under contract Ecou-Pref 'Ecoulements préférentiels dans les versants marneux' (05-ECCO-007-04).

REFERENCES

- Abellan, A., Vilaplana, J.M., Martinez, J., 2006. Application of a long-range Terrestrial Laser Scanner to a detailed rockfall study at Vall de Nuria (Eastern Pyrenees, Spain). *Engineering geology*, Vol. 88(3-4), pp. 136-148.
- Baratoux D., Delacourt C., and Allemand P., 2001. High Resolution Digital Elevation Model derived from Viking images: New method and comparison with MOLA data. *Journal of Geophysical Research*, Vol. 106, No. E12, pp. 32, 927.
- Conforti, D., Deline, P., Mortara, G., Tamburini, A., 2005. Report on the Joint ISPRS Commission VI, Workshop "Terrestrial scanning lidar technology applied to study the evolution of the ice-contact Miage Lake (Mont Blanc, Italy). http://www.innovmetric.com/Surveying/english/pdf/miage_lake.pdf (accessed 11 Jan. 2008).
- Delacourt C., Allemand P, Casson B., and Vadon H., 2004. Velocity field of the "La Clapière" landslide measured by the correlation of aerial and QuickBird satellite images. *Geophysical Research Letters*, Vol. 31, No. 15, L15619, 10.1029/2004GL020193.
- Flageollet, J.-C., Maquaire, O., Weber, D., 1999. Landslides and climatic conditions in the Barcelonnette and Vars basins (Southern French Alps, France). *Geomorphology*, 30, pp. 65-78.
- Kääb A., 2002. Monitoring high-mountain terrain deformation from repeated air- and spaceborne optical data: examples using digital aerial imagery and ASTER data. *ISPRS Journal of Photogrammetry & Remote Sensing*, 57, pp. 39-52.
- Malet, J.P., Maquaire, O., Calais, E., 2002. The use of Global Positioning System for the continuous monitoring of landslides. Application to the Super Sauze earthflow (Alpes-de-Haute-Provence, France). *Geomorphology*, 43, pp33-54.
- Malet, J-P. and Maquaire, O., 2003. Black Marls earthflows mobility and long-term seasonal dynamic in south eastern France). In Picarelli, L. (Ed): *Proceedings of the International Conference on Fast Slope Movements: Prediction and Prevention for Risk Mitigation*, Napoli, Italy, Patron Editore, Bologna, pp. 333-340.
- Monserat, O. and Crosetto, M., 2008. Deformation measurement using terrestrial laser scanning data and least squares 3D surface matching. *ISPRS Journal of Photogrammetry and Remote Sensing*, 63(1), 142-154.
- Oppifer, T., Jaboyedoff, M., Blikra, L.H., Derron, M.-H., 2008. Characterization and monitoring of the Aknes Rockslide using terrestrial laser scanning. 4th Geohazards Canadian Congress, University of Laval, Quebec, 20-24 May 2008.
- Rosser, N.J., Petley, D.N., Dunning, S.A., Lim, M. and Ball, S., 2007. The surface expression of strain accumulation in failing rock masses. In: Eberhardt, E., Stead, D. and Morrison, E. (Editors), *Rock mechanics: Meeting Society's challenges and demands. Proceedings of the 1st Canada-U.S. Rock Mechanics Slob, S. and Hack, R. 2004. 3D Terrestrial Laser Scanning as a New Field Measurements and Monitoring Technique. In Hack, R., Azzam, R. and Charlier, R. (Ed): Engineering Geology for Infrastructure Planning in Europe. A European Perspective. Lecture Note in Earth Sciences. Springer, Berlin / Heidelberg, pp. 179-190.*
- Stephens, R., 2000. *Three-Dimensional Transformations, Visual Basics Graphics Programming*. John Wiley & Sons, New York, pp. 419-464.
- Vadon, H. and Massonnet, P., 2000. Earthquake displacement fields mapped by very precise correlation. Complementarity with radar interferometry, *International Geoscience and Remote Sensing Symposium*, 2000, Vol. 6, pp. 2700-2702, Institute of Electrical and Electronics Engineers, New York, NY, 2000.
- Van Puymbroeck N., Michel R., Binet, R., Avouac, J. P., Taboury J., 2000. Measuring earthquakes from optical satellite images. *Applied Optics*, 39, pp. 3486-3494.